Science Press

ARTICLE

Effect of Calcium on Microstructure, Texture and Mechanical Properties of Mg-4Zn Alloy

Liu Chunquan[1],   Chen Xianhua[1,2],   Chen Jiao[1],   Zhao Chaoyue[1],   Dai Yan[1],
Liu Xiaofang[1],   Zhao Di[1],   Luo Zhu[1],   Tu Teng[1],   Pan Fusheng[1,3]

[1] International Joint Laboratory for Light Alloys (Ministry of Education), Chongqing University, Chongqing 400045, China; [2] National Engineering Research Center for Magnesium Alloys, Chongqing 400044, China; [3] Chongqing Academy of Science and Technology, Chongqing 401123, China

Abstract: The effect of calcium (Ca) additions on microstructure, texture and mechanical properties of Mg-4Zn alloy was investigated. The as-cast alloys consisted of α-Mg dendrites and MgZn phase, and Ca addition also caused the formation of ternary $Ca_2Mg_6Zn_3$ phase. Results show that Ca element significantly refines the grain size of extruded sheet and weakens the strong basal textures. Along the transverse direction (TD) of the sheet, Mg-4Zn-0.3Ca alloy exhibits an ultimate tensile strength (UTS) of 260 MPa and a tensile yield strength (TYS) of 163 MPa. Moreover, the elongation to failure of Ca containing alloy increases up to 24% compared to that of 19% for Mg-4Zn alloy. The recrystallization mechanism and texture evolution of the alloy were analyzed. In addition, the strengthening and toughening mechanism, including the anisotropy of mechanical characteristics, both were studied.

Key words: magnesium alloys; dynamic recrystallization; texture; anisotropy

Mg-Zn series alloy is one of the most widely used wrought magnesium alloys because of its combination of lightweight with high specific strength and low cost. However, currently the application of Mg-Zn binary alloy is limited by the large crystallization temperature interval and the bad liquidity. What's more, zinc easily leads to microporosity and hot cracking tendency[1]. Therefore, it is necessary to add other elements into the Mg-Zn alloy to improve the microstructure and properties[2].

Among the various ways that has been tried to improve the formability of magnesium alloys by modifying their structure, the addition of rare-earth (RE) alloy elements, such as Y, Ce, La, Nd was investigated[3-7]. Although the effect of rare-earth (RE) elements on improving the microstructure and properties of magnesium alloy is quite remarkable, the distinct disadvantage of RE elements is the high cost. Therefore, it is necessary to research other replaceable alloying elements which have similar effects on

microstructure and mechanical properties compared to RE elements[8-10]. Ca belongs to alkali earth metals, whose density (about 1550 kg/m^3) is close to that of magnesium and whose price is low. In addition, many studies show that, Ca has many similar characteristics to rare earth elements, such as effectively refining the grain size, modifying the corrosion resistance of Mg alloys due to the formation of an oxide layer, weakening the basal texture, enhancing high temperature stability[11-16]. Besides, both Ca and Zn can be well metabolized by the human body. Therefore, the Mg-Zn-Ca series alloy has great potential in biomedical applications[17]. Recently, Ca containing series alloy has motivated increasing interest. But, Zn content exceeding 4.0 wt% causes coarsening of the microstructure of Mg-Zn-Ca series alloy, which is unbeneficial to the comprehensive mechanical properties[11]. And addition of even a small amount of Ca 0.3 wt%~0.4 wt% to Mg-Zn alloys results in significant grain refinement[13]. Although the addition of Ca

element is quite remarkable to improve the comprehensive mechanical properties of Mg-Zn alloys, many aspects, such as texture modification, the strengthening and toughening mechanism, and the anisotropy of Mg-Zn-Ca alloys, were not studied systematically[18, 19].

Based on the existing researches, this work studied the influence of Ca element on the microstructure, mechanical properties and anisotropy of Mg-4Zn alloys. The recrystallization mechanism and texture evolution were discussed.

1 Experiment

Two alloys with nominal chemical composition of Mg-4Zn and Mg-4Zn-0.3Ca (wt%) were studied in this work. Alloys were melted in an induction heated iron crucible and protected by a gas mixture consisting of CO_2 (99.99 vol%) and SF_6 (1 vol%). Mg-20Ca (wt%) master alloy, pure Mg (99.85 wt%), Zn (99.90 wt%) were used in the present work. Melted alloys were kept for about 15 min at 720 ^{o}C to ensure that all alloying elements dissolved in the melt. Subsequently melted alloys were poured into a stainless steel mold.

Afterwards, the as-cast ingots were homogenized at 300 ^{o}C for 5 h and 400 ^{o}C for 16 h followed by water quenching (25 ^{o}C). The extrusion process was carried out XJ-500 Horizontal Extrusion Machine with 500 t, and these homogenized ingots were extruded at 400 ^{o}C under an extrusion ratio of 25:1 and a die-exit speed of 1.7×10^{-2} m/s. Samples machined from the cast ingot and extrusion plate were etched in a picric acid solution containing 1.0 g picricacid, 20 mL ethanol, 2 mL acetic acid, and 2 mL distilled water. Then, the microstructures of the as-cast and as-extruded alloys were examined in a ZEISS NEOPHOT 30 optical microscope (OM). Preliminary examination of phases in the as-cast alloys was done by a Rigaku D/MAX-2500PC X-ray diffractometer (XRD). The detailed studies of distribution and types of phases were done by a TESCAN VEGAⅡLMH scanning electron microscope (SEM) equipped with an INCA Energy 350 energy-dispersive X-ray spectrometry system (EDS). Texture measurement of the extrusion plate was performed by XRD. The tensile tests were carried out at room temperature by a SANSIU CMT-5105 instrument at a strain rate of 1.0×10^{-3} s^{-1}. The tensile yield strength (YS), ultimate tensile strength (UTS) and elongation to fracture (FE) are the average values of three individual repeated tests at least. Thus, bone like tensile specimens having a gage length of 45 mm and gage width of 10 mm were taken from three orientations: α=0°, 45°, 90° as shown in Fig.1.

2 Results and Discussion

2.1 Microstructure

The XRD patterns of as-cast Mg-4Zn and Mg-4Zn-0.3Ca alloys, as shown in Fig.2, indicate that two samples are

Fig.1 Schematic diagram of Mg-Zn-Ca alloy sheets sampling sites for stretched specimen (ND: normal direction, ED: extruded direction, TD: transverse direction)

mainly composed of α-Mg matrix and a few second phases MgZn, while the second phase $Ca_2Mg_6Zn_3$ is only detected in Mg-4Zn-0.3Ca alloy. Optical micrographs and SEM images of as-cast Mg-4Zn and Mg-4Zn-0.3Ca alloys are illustrated in Fig.3. It can be observed that two as-cast alloys both exhibit a large grain size, and many irregular granular second phases are located in grains or grain boundaries. After the addition of Ca element, the number of the second phase increases and the second phases located at the grain boundaries gradually become a continuous network structure. Magnified SEM images of as-cast Mg-4Zn and Mg-4Zn-0.3Ca alloys are shown in the right corner (Fig.3c and 3d). It can be seen that the second phases in both alloys exhibit two morphologies: spherical and irregular bulk. EDS and XRD analyses reveal that these second phases in Mg-4Zn alloy are MgZn, but in Mg-4Zn-0.3Ca alloy, they are $Ca_2Mg_6Zn_3$ and MgZn.

As shown in Fig.4, after homogenization, the second phase in Mg-4Zn alloy mainly dissolves into magnesium matrix, leaving only a few second phase particles with a size of 5~20 μm. But in Ca-containing alloy, only part of the second phase dissolves into the magnesium matrix after the homogenization treatment, and some second phase with a mean particle size of 6~44 μm remains.

The microstructures of as-extruded Mg-4Zn and Mg-4Zn-0.3Ca alloys are shown in Fig.5. It can be observed that
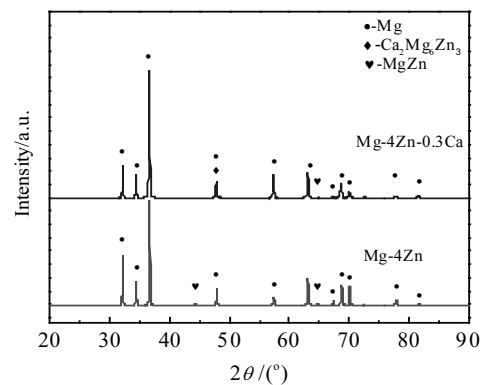

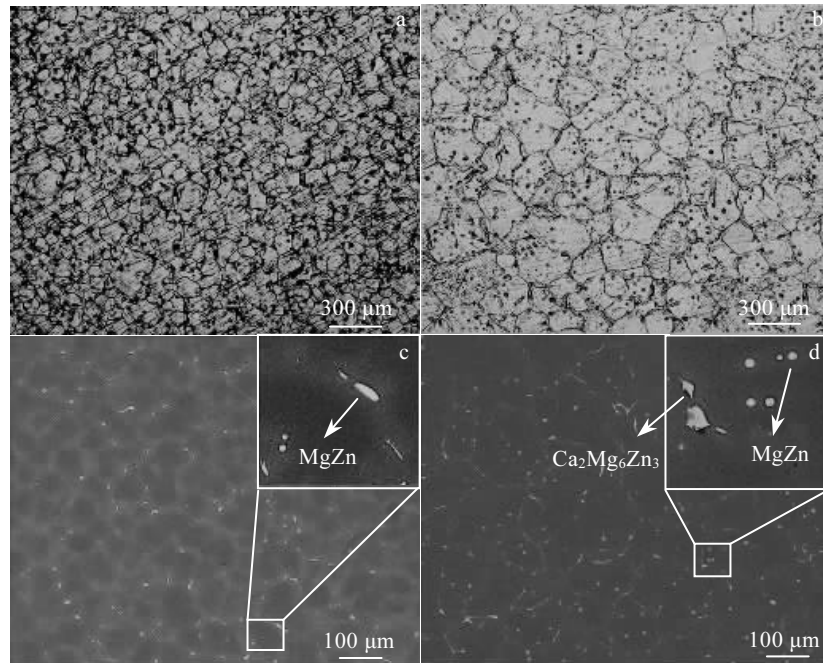Fig.2 XRD patterns of as-cast Mg-4Zn and Mg-4Zn-0.3Ca alloys

Fig.3   OM (a, b) and SEM (c, d) images of as-cast Mg-4Zn (a, c) and Mg-4Zn-0.3Ca (b, d) alloys
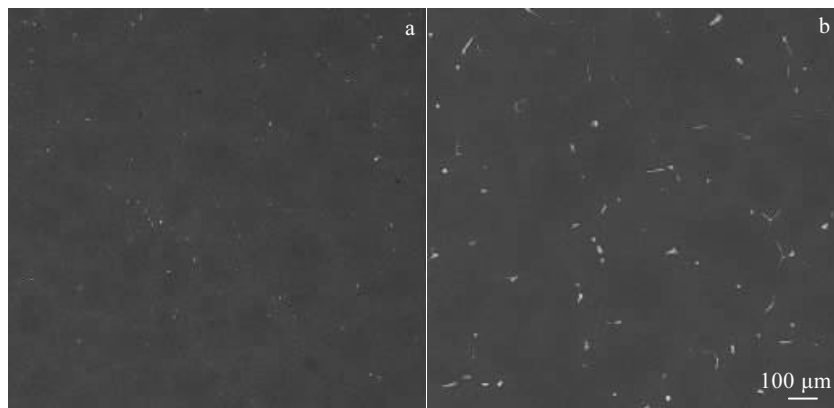
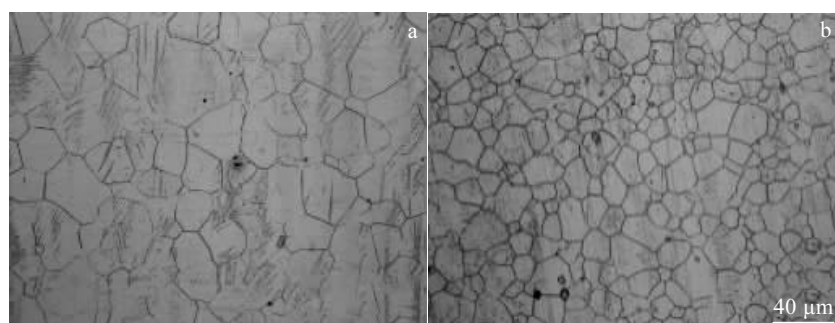Fig.4   SEM images of as-homogenized Mg-4Zn (a) and Mg-4Zn-0.3Ca (b) alloys

Fig.5   OM images of as-extruded Mg-4Zn (a) and Mg-4Zn-0.3Ca (b) alloy sheets

that the grain size of two alloys decreases significantly after extrusion, and the grains are relatively homogeneous. This shows that fully dynamic recrystallization occurs during the hot extrusion process. However, some large grains still exist in both alloys, which is probably due to the higher extrusion temperature (400 ^{o}C) resulting in the growth of partially recrystallized grains. Meanwhile, it is also found that in the as-extruded sheets, there are some little precipitate particles which can prevent dynamic recovery and dynamic recrystallization[17]. These small amounts of fine precipitates act as pinning points to the grain boundaries, effectively preventing the boundaries migration and the growth of recrystallized grains, and finally refining the grains. Table 1 summarizes the grain size of as-extruded of two alloys. The average grain size of as-extruded Mg-4Zn-0.3Ca alloy is obviously smaller than that of Mg-4Zn alloy, which show that the grain size of extruded alloy is obviously refined after adding Ca.

Dynamic recrystallization (DRX) always occurs during the thermal deformation. The typical mechanisms of dynamic recrystallization of magnesium alloys includes: (a) strain-induced boundary migration (SIBM); (b) continuous dynamic recrystallization (CDRX); (c) discontinuous dynamic recrystallization (DDRX) and so on. Particle-stimulated nucleation (PSN) is one of important nucleation mechanism of magnesium alloy in DRX process. The influence of large particles on increasing recrystallization fraction via the mechanism of PSN is well known. During the hot-extrusion deformation, deformation zones are formed around the large (>1 μm diameter) and brittle second-phase particles. Dynamic response occurs in these deformation zones, resulting in the formation of a large number of sub-boundaries. As the deformation proceeds, the thermal activation energy increases continuously, and the sub-boundaries expand continuously, and then transform into high angle grain boundaries (HAGBs) when the difference in orientation accumulates to a sufficient degree[20]. Afterwards, a new grain nucleus is produced, which grows into a recrystallized grain. An important feature of PSN-nucleated grains is that their orientations are different from those formed by other recrystallization mechanisms. Because of this, PSN can also improve the texture of the alloy[20]. As shown in Fig.4, part of the second phase of the Mg-4Zn-0.3Ca alloy is dissolved into the magnesium matrix after the homogenization treatment, but with a mean particle size larger than the critical particle size (1 μm) of PSN remains. The Ca-containing alloy used in this study

contains coarse particles which can provide the PSN sites to produce more grain nucleus, so the PSN mechanism effect in Mg-4Zn-0.3Ca alloy is remarkable. After homogenization, the second phase of Mg-4Zn alloy is mainly dissolved into the magnesium matrix, leaving only few second phase particles with a size of 5~20 μm. However, the conditions of PSN mechanism include not only the critical particle size, but also the critical strain levels. During hot extrusion, the second phase MgZn which owns a low melting point and poor thermal stability, precipitates in Mg-4Zn alloy. It cannot accumulate enough strain around the second phase during deformation, so the PSN mechanism effect in Mg-4Zn alloy is not as significant as that in Mg-4Zn-0.3Ca alloy.

2.2 Texture

The texture data are examined in the form of pole figures, and the typical textures of two alloys are shown in Fig.6. In two cases, the pole density is tilted away from the sheet normal direction (ND) toward to the ED by a certain angle, and with the addition of 0.3 wt% Ca element, the basal texture of Mg-4Zn alloy effectively weakens from 15.9 to 6.7. But the orientation of prismatic plane (10$\bar{1}$0) in two alloys is relatively random. The main feature of the texture with the Ca addition seems like the splitting of basal poles. As shown in Fig.6b, Mg-4Zn-0.3Ca alloy has lower basal pole intensity parallel to the sheet ND. The highest intensity pole is separated into three points distributing along the ED direction. Fig.7 shows the effect of Ca element on the grain orientation in the extruded sheet. The basal plane (0001) of most grains is parallel to the extruded surface which forms a strong basal texture. The *c*-axis of few grains is offset by an angle α along the ED direction in Mg-4Zn alloy. With the addition of Ca, the *c*-axis of grains deflects more obviously along the ED direction, $\beta > \alpha$, which make the grain orientation more random and weaken the intensity of basal texture. This morphology is similar to that of the wrought magnesium alloys containing rare earths, such as Gd and Ce[21-23].

The previous results show that the texture improvement caused by Ca seems to be the influence of Ca addition on dynamic recrystallization. Therefore, this paragraph would like to discuss the mechanism of the texture modification. From the foregoing analysis of the dynamic recrystallization of the extruded alloy, PSN is an important nucleation mechanism of Mg-4Zn-0.3Ca alloy. In addition, as shown in Fig.5, some submicron precipitates are dispersed within the grains and boundaries, which could effectively refine the recrystallized grains. What's more, the random grain orientation is beneficial to weakening the basal texture in the alloy, and then improving the plastic deformation capacity of the alloy[24, 25]. It can be seen that the effect of the PSN mechanism and precipitation phase is an important reason for weakening of the basal texture in these alloys.

Table 1   Grain size of as-extruded Mg-Zn-Ca alloys

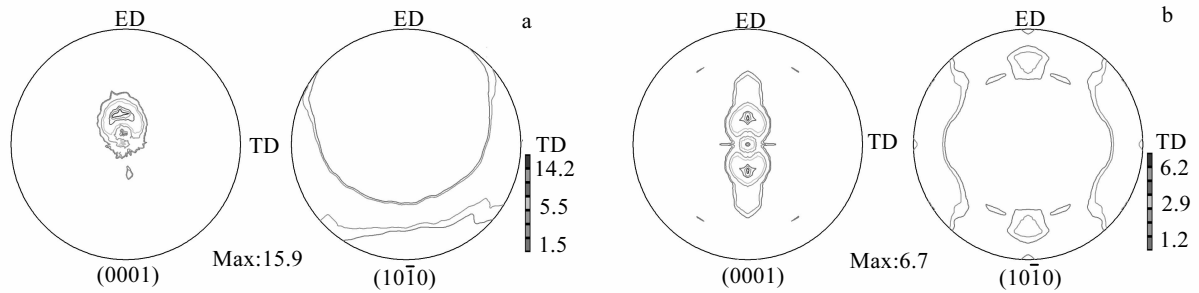| Alloy	Grain size/μm
Mg-4Zn	24
Mg-4Zn-0.3Ca	12

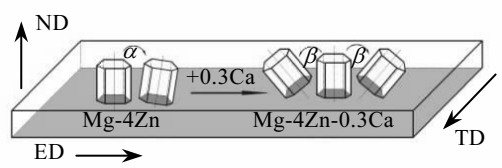Fig.6   Pole figures of as-extruded Mg-4Zn (a) and Mg-4Zn-0.3Ca (b)

Fig.7   Comparison of grain orientation between Mg-4Zn and Mg-4Zn-0.3Ca

Except the PSN mechanism effect, from the above experimental results of alloy microstructure, it can be seen that a large amount of Zn and Ca elements in Mg-4Zn-0.3Ca alloy are solid dissolved in the magnesium matrix after extrusion. It has been confirmed that the solid solution alloy element may change the stacking fault energy (SFE) which can influence the dynamical recrystallization process and further influence the texture of alloy[23, 25, 26]. However, the maximum solubility of Ca in magnesium at room temperature is 0.2 wt%. In this work, the content of Ca is only within 0.3 wt%. It can be seen that the solid solubility of two alloying for texture modification is not significant. Except the stacking fault energy, the axial ratio (c/a) value also affects the dislocation slip and the texture evolution[27, 28]. As shown in Table 2, the c/a values of pure magnesium, Mg-4Zn and Mg-4Zn-0.3Ca alloys are 1.6236, 1.6240 and 1.6218. It is found that Ca could slightly reduce the axial ratio, so the effect of c/a values on texture modification is not remarkable. According to above analysis, the stacking fault energy and c/a value are very essential physical properties of magnesium alloy, which not only affect the start of the basal plane slip but also influence the texture indirectly, then improving the plastic deformation capacity of magnesium alloy.

Table 2   *c/a* ratio of magnesium, Mg-4Zn and Mg-4Zn-0.3Ca alloys

Material	Mg	Mg-4Zn	Mg-4Zn-0.3Ca
c/a ratio	1.6236	1.6240	1.6218

2.3   Mechanical properties

From Fig.8, it can be clearly observed that the highest tensile yield strength (TYS) of two alloys is measured along TD and the lowest along ED. Overall, the TYS of Mg-4Zn-0.3Ca alloy in all directions is slightly higher than that of Mg-4Zn alloy. It can be seen from Table 3 that with the addition of Ca, the ultimate tensile stress (UTS) of Mg-4Zn alloy increases from 245 MPa to 260 MPa along TD direction and the rest direction also increases to some extent. It is worth mentioning that the addition of Ca results in a significant improvement in the elongation of the alloy. The elongation to failure along the ED of Mg-4Zn-0.3Ca alloy reaches to 27%, which is 5% higher than that of Mg-4Zn alloy. The elongation in each direction is not much different, which indicates that the anisotropy of alloy is not significant.

The anisotropy of magnesium alloy sheet has an important influence on secondary plastic forming. The thickness anisotropic index of the plate r is different in three directions, and the anisotropy of the plate could be represented by Δr[29]:

$$r = \frac{\varepsilon_b}{\varepsilon_t} = \frac{\ln b / b_0}{\ln t / t_0} \tag{1}$$

$$\Delta r = \frac{1}{2}\left| r_0 - r_{90} - r_{45} \right| \tag{2}$$

where b_0 is the width of the sheet before stretching, b is the width of the sheet after stretching, t_0 is the thickness of the sheet before stretching, t is the thickness of the sheet after stretching. Larger r value shows that the strain in the width direction is larger than thickness direction when the material undergoes tensile deformation, which means that the thickness of the material is difficult to change. Larger Δr value indicates the anisotropy of the sheet is more serious, the second deformation would form lugs, which directly affect the quality of secondary forming parts and the material utilization. Typical stress-strain curves from tensile tests are shown in Fig.8 for ED, 45°, and TD. The curve intervals between three directions both exist in two alloys, but the interval in the
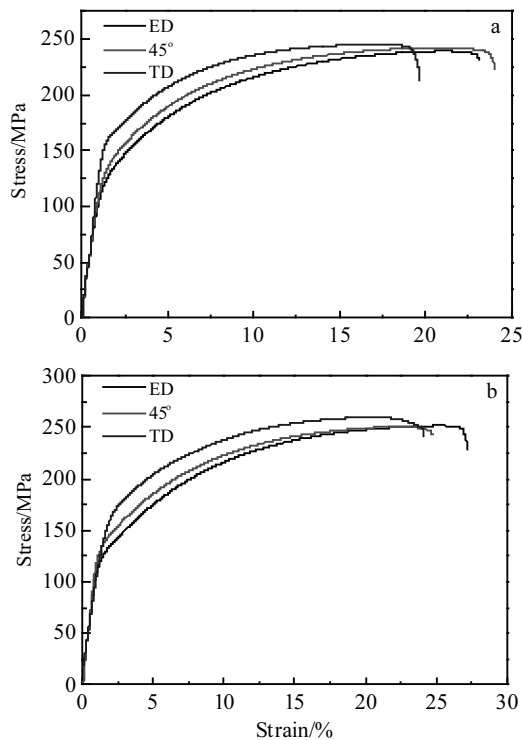
Fig.8 Anisotropy engineering stress-strain curves of as-extruded Mg-4Zn (a) and Mg-4Zn-0.3Ca (b) alloy

Ca-containing alloy is smaller than that of Mg-4Zn alloy. The anisotropy indices Δr-values of the two alloys in Table 3 are 0.54 and 0.39, respectively, which shows that the addition of Ca decreases the anisotropy of the Mg-Zn alloy to some extent.

The mechanisms of strengthening in two alloys are discussed in these paragraphs. Typical mechanisms of strengthening in magnesium alloy include: grain refinement reinforcing, dispersal reinforcing, solid-solution strengthening, and texture strengthening etc. According to Hall-Petch[30] relationship:

$$\sigma_y = \sigma_0 + k_y d^{1/2} \tag{3}$$

Where σ_y is the yield strength (N/m^2), σ_0 is the friction stress when dislocation glides on the slip plane (N/m^2), σ_y is the locking parameter representing grain boundaries as an obstacle to slip (N/m$^{3/2}$), d is the average grain size. Grain refinement could be an effective way for enhancing the strength of magnesium alloy. Moreover, the activation of twinning and slips is affected by microstructure, temperature and strain rate. Compared with fcc and bcc metals, magnesium alloys has a complex deformation behavior due to the hcp structure[31]. Actually, the operation of twinning or dislocation slip is closely linked to the value of critical resolved shear stresses (CRSS). The basal <a> slip has the lowest CRSS at room temperature.

As long as the resolved shear stress reaches the CRSS, the dislocation can be activated. But grain boundaries (GBs) can block the movement of dislocation, and then lead to the stress concentration at grain boundaries due to the GBs effect[32-34]. The propagation of dislocation slip from one grain to a neighbor grain relies on both the stress concentration created by GBs effect and the externally applied stress. The stress concentration aroused by GBs in coarse grain is bigger than in small one, so that the larger external stress is required in small grains to activate the dislocation source in adjacent grains, which improves the plastic deformation resistance. As shown in Fig.5, the grain size is significantly refined after the addition of Ca element, corresponding mechanical properties are improved, so the grain refining effect produced by Mg-4Zn-0.3Ca is more pronounced than that of the Mg-4Zn alloy.

The solubility of Zn in magnesium is 6.2 wt%. It can be seen from Fig.5 that less second phase precipitates in the extruded sheet, so it is presumed that a mass of Zn element is dissolved in the magnesium matrix resulting in solid solution strengthening. In particular, Mg-4Zn alloy has the strongest effect of solid solution strengthening. Because Mg-4Zn-0.3Ca alloy consumes part of Zn involved in the formation of Ca$_2$Mg$_6$Zn$_3$ phase, the solid solution strengthening effect is relatively weak. The solubility of Ca in magnesium is only 0.82 wt% at 516.5 ^{o}C[9], so the solid solution strengthening effect is not obvious and is not considered here. It can be observed from Fig.5 that submicron precipitates are precipitated in both alloys dispersedly, but the amount of them is not enough to arouse the dispersion strengthening, so the dispersion strengthening effect is also limited.

Fig.6 shows that the basal texture of the Mg-4Zn alloy is strong. Intense basal texture is beneficial to tensile strength but harmful to ductility of the alloy, and the crystalline orientation controls the difficulty degree of plastic deformation. As observed from Fig.7, the basal plan of most grain is parallel to extruded surface, which shows a typical hard-orientation, only a few grains are offset by an angle along the ED direction. With the addition of Ca, the spilt angle in Mg-4Zn-0.3Ca alloy is more obvious than in Mg-4Zn, which makes the grain orientation more random and transfrom hard-orientation to soft-orientation which is attributed to plastic deformation. At room temperature, the main deformation mechanism in magnesium alloy is (0001)<11$\bar{2}$0> which has two independent slip systems[35]. The more random grain orientation is beneficial to activation of the basal slip (0001)<11$\bar{2}$0>, so the plasticity of Mg-4Zn-0.3Ca alloy is improved. Although the weakened texture is harmful to tensile strength, the strengthening effect aroused by fine crystal reinforcing is dominant. Thus, the Mg-4Zn-0.3Ca

Table 3   Mechanical properties and anisotropy factor of Mg-Zn-Ca alloy sheets

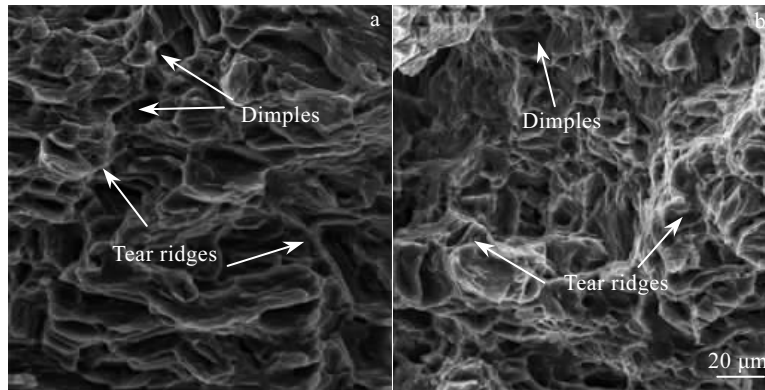| Alloy	Angle/(°)	TYS/MPa	UTS/MPa	Elongation/%	r	△r
	0	117	240	22.8	1.52	
Mg-4Zn	45	130	242	24	2.28	0.54
	90	158	245	19	4.13	
	0	121	252	27	1.93	
Mg-4Zn-0.3Ca	45	135	250	24.7	2.56	0.39
	90	163	260	24	3.96	

Fig.9   SEM images of the fracture surfaces of as-extruded Mg-4Zn (a) and Mg-4Zn-0.3Ca (b) alloy

alloy exhibits favorable comprehensive mechanical properties in the end.

The fracture surfaces of tensile specimens are shown in Fig.9. There are some dimples and tear ridges in the fracture surface of Mg-4Zn alloy (seen Fig.9a), which shows the characteristics of plastic fracture. The number of dimples in Mg-4Zn-0.3Ca alloy is more intensive with fewer tear ridges (seen Fig.9b). So, the alloy exhibits better tensile plasticity than Mg-4Zn. From the above experimental results, the strengthening mechanism of Mg-4Zn alloy mainly includes fine crystal reinforcing, solid solution strengthening and texture strengthening. Fine crystal reinforcing could be the main mechanism in Mg-4Zn-0.3Ca alloy.

3   Conclusions

1) Two investigated alloys have revealed α-Mg matrix with the second phases distributed in grains or grain boundaries. The MgZn phase is identified as the main intermetallic phase in Mg-4Zn and Mg-4Zn-0.3Ca alloys. Apart from MgZn phase, Ca addition causes the formation of ternary $Ca_2Mg_6Zn_3$ phase.

2) The Ca-containing alloy contains coarse particles $Ca_2Mg_6Zn_3$ which can provide the PSN sites to produce more grain nucleus and cause the grain refinement and texture improvement.

3) The addition of low content of Ca element strongly weakens the texture intensity of Mg-4Zn alloy from 15.9 to 6.7. The as-extruded Mg-4Zn-0.3Ca sheet shows a typical texture structure having a splitting of basal poles toward the extruded direction.

4) With the addition of Ca element, tensile yield strength increases from 158 to 163 MPa, ultimate tensile strength increased from 245 to 260 MPa, and elongation increases from 19% to 24% in transverse direction. What's more, the anisotropy of the plate defined by Δr decreases from 0.54 to 0.39. The comprehensive mechanical properties of Mg-4Zn alloy are improved to some extent.

References

1 Wei L Y, Dunlop G L, Westengen H. *Metallurgical & Materials Transactions A*[J], 1995, 26(7): 1705

2 Bhattacharjee T, Mendis CL, Oh-Ishi K *et al. Materials Science and Engineering A*[J], 2013, 575(28): 231

3 Liu H, Huang H, Yang X *et al. Journal of Magnesium & Alloys*[J], 2017, 5(2): 231

4 Liu L, Chen X, Pan F *et al. Journal of Alloys & Compounds*[J], 2016, 688: 537

5 Huang D, Chen Y, Tang Y *et al. Rare Metal Materials and Engineering*[J], 2006, 35(12):1864

6 Fang X, Wu S, Zhao L *et al. Rare Metal Materials and Engineering*[J], 2016, 45(1): 7

7 Liu L, Chen X, Pan F *et al. Materials Science and Engineering A*[J], 2015, 644: 247

8 Kim D W, Suh B C, Shim M S *et al. Metallurgical & Materials Transactions A*[J], 2013, 44(7): 2950

9 Guo F, Feng B, Fu S *et al. Journal of Magnesium & Alloys*[J], 2017, 5(1): 13

10 Hono K, Mendis C L, Sasaki T T *et al. Scripta Materialia*[J], 2010, 63(7): 710

11 Hradilová M, Montheillet F, Fraczkiewicz A *et al. Materials Science and Engineering A*[J], 2013, 580(10): 217

12 Yang M, Guo T, Li H. *Materials Science and Engineering A*[J], 2013, 587(12):132

13 Naghdi F, Mahmudi R, Kang J Y *et al. Materials Science and Engineering A*[J], 2016, 649: 441

14 Tong L B, Zheng M Y, Cheng L R *et al. Materials Science and Engineering A*[J], 2013, 569(3): 48

15 Levi G, Avraham S, Zilberov A *et al. Acta Materialia*[J], 2006, 54(2): 523

16 Oh J C, Ohkubo T, Mukai T *et al. Scripta Materialia*[J], 2005, 53(6): 675

17 Hradilová M, Vojtěch D, Kubásek J *et al. Materials Science and Engineering A*[J], 2013, 586(8): 284

18 Yang M, Liu D, Zhang R *et al. Rare Metal Materials and Engineering*[J], 2018, 47(1): 93

19 You S, Huang Y, Kainer K U *et al. Journal of Magnesium & Alloys*[J], 2017, 5(3): 239

20 Robson J D, Henry D T, Davis B. *Acta Materialia*[J], 2009, 57(9): 2739

21 Liu P, Jiang H, Cai Z *et al. Journal of Magnesium & Alloys*[J], 2016, 4(3): 188

22 Stanford N, Barnett M R. *Materials Science and Engineering A*[J], 2008, 496(1): 399

23 Ding H L, Zhang P, Cheng G P *et al. Transactions of Nonferrous Metals Society of China*[J], 2015, 25(9): 2875

24 Stanford N. *Materials Science and Engineering A*[J], 2010, 528(1): 314

25 Zhang B, Wang Y, Geng L *et al. Materials Science and Engineering A*[J], 2012, 539(2): 56

26 Chino Y, Huang X, Suzuki K *et al. Materials Transactions*[J], 2010, 51(4): 818

27 Ding H, Shi X, Wang Y *et al. Materials Science and Engineering A*[J], 2015, 645: 196

28 Tong L B, Zheng M Y, Cheng L R *et al. Materials Characterization*[J], 2015,104: 66

29 Bohlen J, Nürnberg M R, Senn J W *et al. Acta Materialia*[J], 2007, 55(6): 2101

30 Yu H, Li C, Xin Y *et al. Acta Materialia*[J], 2017, 128: 313

31 Wang X J, Xu D K, Wu R Z *et al. Journal of Materials Science & Technology*[J], 2018, 34(2): 245

32 Hall E O. *Proceedings of the Physical Society*[J], 2002, 64(6): 495

33 Petch N J. *J Iron Steel Inst*[J], 1953, 174(1): 25

34 Armstrong R, Codd I, Douthwaite R M *et al. Philosophical Magazine*[J], 1962, 7(73): 45

35 Alaneme K K, Okotete E A. *Journal of Magnesium & Alloys*[J], 2017, 5(4): 460

钙对 Mg-4Zn 合金组织、织构及力学性能的影响

刘春全[1]，陈先华[1,2]，陈　娇[1]，赵超越[1]，代　言[1]，刘晓芳[1]，赵　娣[1]，罗　铸[1]，涂　腾[1]，潘复生[1,3]

(1. 重庆大学 轻合金国际联合实验室(教育部)，重庆 400045)

(2. 国家镁合金工程技术研究中心，重庆 400044)

(3. 重庆市科学技术研究院，重庆 401123)

摘　要：研究了钙对 Mg-4Zn 合金组织、织构及力学性能的影响。铸态 Mg-4Zn 合金包含 α-Mg 相和 MgZn 相，Ca 的加入还生成了 $Ca_2Mg_6Zn_3$ 三元相。结果表明，Ca 显著细化挤压板材的晶粒尺寸，弱化板材织构。沿着板材横向，Mg-4Zn-0.3Ca 合金的屈服强度为 163 MPa，最终抗拉强度达到 260 MPa。并且，加钙后合金延伸率从 Mg-4Zn 合金的 19%提高到 24%。分析了合金的再结晶机制，织构演变机理和强韧化机制，另外，合金力学性能与各向异性也得到了分析。

关键词：镁合金；动态再结晶；织构；各向异性

作者简介：刘春全，男，1995 年生，硕士，重庆大学材料科学与工程学院，重庆 400045，电话：023-65102366，E-mail: cqliu@cqu.edu.cn